Optica Applicata, Vol. XL, No. 4, 2010

High focusing of radially polarized Bessel-modulated Gaussian beam

XIUMIN GAO[1, 2*], MINGYU GAO[1], SONG HU[1], HANMING GUO[2], JIAN WANG[1], SONGLIN ZHUANG[2]

[1]Electronics and Information College, Hangzhou Dianzi University, Hangzhou 310018, China

[2]University of shanghai for Science and Technology, Shanghai 200093, China

[*]Corresponding author: xiumin_gao@yahoo.com.cn

The focusing properties of radially polarized Bessel-modulated Gaussian (QBG) beam are theoretically investigated in detail by vector diffraction theory. The QBG beam contains an optical vortex. Calculation results show that the intensity distribution in focal region of radially polarized QBG beam can be altered considerably by changing beam parameter and the topological charge of the optical vortex. Beam parameter can induce remarkable focus evolution in axial direction. While topological charge adjusts intensity distribution more significantly in transverse direction, for instance, one focal spot changes into one ring pattern. And some novel focal patterns may occur, including two-peak focus, one ring focus, two-ring focus, three-ring focus, and even dark hollow focus, which is very important in optical tweezers technique.

Keywords: focusing properties, Bessel-modulated Gaussian beam, vector diffraction theory.

1. Introduction

Since Caron and Potvliege introduced the Bessel-modulated Gaussian (QBG) beams with quadratic radial dependence, QBG beams have attracted much attention [1–7]. It was shown that such a class of beams has familiar collinear geometry of the Gaussian beam and also has an interesting non-Gaussian feature for certain values of its parameters [1–3]. Belafhal and Dalil-Essakali studied the propagation properties of QBG beams through an unapertured optical paraxial ABCD system [4]. Wang and Lü conducted research into the beam propagation factor, far-field distribution, and the kurtosis parameter of such type of beams [3, 5, 6]. The Bessel-modulated Gaussian light beams passing through a paraxial ABCD optical system with an annular aperture has also been studied [7]. Hricha and Belafhal investigated in detail the focusing properties and focal shift of the axisymmetric QBG beam passing through a non--apertured aberration-free lens [2]. Polarization plays an important role in many optical systems, and can be used to alter propagating and focusing properties of light beam. For example, laser beam with cylindrical symmetrical polarization has recently attracted many researchers because the electric field in focal region of such cylindrical

vector beam has some unique properties [8–11]. In addition, in high numerical aperture optical systems, vector diffraction theory is employed to replace scalar diffraction theory to provide more accurate results. The present paper is aimed at studying theoretically focusing properties of the radially polarized QBG beam by vector diffraction theory. The principle of the focusing radially polarized QBG beam is given in Section 2. Section 3 gives the simulation results and discussion. The conclusions are summarized in Section 4.

2. Principle of the focusing radially polarized QBG beam

In the focusing system we investigated, the focusing beam is a radially polarized QBG beam whose value of transverse optical field is the same as that of the scalar QBG [1–3], and its polarization distribution turns on radial symmetry [10, 11]. Therefore, in the cylindrical coordinate systems $(r, \phi, 0)$, the field distribution $\mathbf{E}(r, \phi, 0)$ of the radially polarized QBG beam in the incident pupil plane is written as

$$\mathbf{E_0}(r, \varphi, 0) = E_0(r, \varphi, 0) \cdot \mathbf{n_r} \tag{1}$$

where $\mathbf{n_r}$ is the radial unit vector of polarized direction. The term $E_0(r, \varphi, 0)$ is the optical field value distribution and can be written in the form [1, 2],

$$E_0(r, \varphi, 0) = C J_{|m|/2}\left(\frac{\mu r^2}{\omega_0^2}\right) \exp\left(-\frac{r^2}{\omega_0^2}\right) \exp(im\varphi) \tag{2}$$

where $J_{|m|/2}$ denotes the Bessel function of order $|m|/2$, ω_0 is the waist width, and μ is a beam parameter which is complex-valued in general. It should be noted that there is one optical vortex on axis, and m is the topological charge of the optical vortex. C is a constant. According to vector diffraction theory, the electric field in focal region of radially polarized QBG beam is [12],

$$\mathbf{E}(\rho, \phi, z) = E_\rho \mathbf{e}_\rho + E_\phi \mathbf{e}_\phi + E_z \mathbf{e_z} \tag{3}$$

where $\mathbf{e}_\rho$, $\mathbf{e}_\phi$, and $\mathbf{e_z}$ are the unit vectors in the radial, azimuthal, and propagating directions, respectively. To indicate the position in image space, cylindrical coordinates $(r, \phi, 0)$ with origin $\rho = z = 0$ located at the paraxial focus position are employed. E_ρ, E_ϕ, and E_z are amplitudes of the three orthogonal components and can be expressed as

$$E_\rho(\rho, \phi, z) = -\frac{iA}{\pi} \int_0^\alpha \int_0^{2\pi} \sqrt{\cos\theta}\, E_0 \sin\theta \cos\theta \cos(\varphi - \phi) \times$$

$$\times \exp\left\{ ik\left[z\cos\theta + \rho \sin\theta \cos(\varphi - \phi) \right] \right\} \mathrm{d}\varphi\, \mathrm{d}\theta \tag{4}$$

$$E_\phi(\rho,\phi,z) = -\frac{iA}{\pi}\int_0^{\alpha}\int_0^{2\pi}\sqrt{\cos\theta}\,E_0\sin\theta\cos\theta\sin(\varphi-\phi)\times \\ \times\exp\left\{ik\left[z\cos\theta+\rho\sin\theta\cos(\varphi-\phi)\right]\right\}\mathrm{d}\varphi\,\mathrm{d}\theta \tag{5}$$

$$E_z(\rho,\phi,z) = \frac{iA}{\pi}\int_0^{\alpha}\int_0^{2\pi}\sqrt{\cos\theta}\,E_0\sin^2\theta\times \\ \times\exp\left\{ik\left[z\cos\theta+\rho\sin\theta\cos(\varphi-\phi)\right]\right\}\mathrm{d}\varphi\,\mathrm{d}\theta \tag{6}$$

where θ denotes the tangential angle with respect to the z axis, and φ is the azimuthal angle with respect to the x axis; k is the wave number; $\alpha = \arcsin(\mathrm{NA})$ is the convergence angle corresponding to the radius of incident optical aperture, where NA is numerical aperture. In order to make the focusing properties clear and simplify calculation process, after simple derivation, Eq. (2) can be rewritten as

$$E_0(\theta,\varphi,0) = C\,J_{|m|/2}\left(\frac{\sin^2\theta}{w^2\mathrm{NA}^2}\right)\exp\left(-\frac{\sin^2\theta}{w^2\mathrm{NA}^2}\right)\exp(im\varphi) \tag{7}$$

where $w = \omega_0/r_0$ is called relative waist width. Substituting Eq. (7) into Eqs. (4)–(6), we can obtain

$$E_\rho(\rho,\phi,z) = -\frac{iAC}{\pi}\int_0^{\alpha}\int_0^{2\pi}\sqrt{\cos\theta}\,\sin\theta\cos\theta\cos(\varphi-\phi)\times \\ \times J_{|m|/2}\left(\frac{\sin^2\theta}{w^2\mathrm{NA}^2}\right)\exp\left(-\frac{\sin^2\theta}{w^2\mathrm{NA}^2}\right)\exp(im\varphi)\times \\ \times\exp\left\{ik\left[z\cos\theta+\rho\sin\theta\cos(\varphi-\phi)\right]\right\}\mathrm{d}\varphi\,\mathrm{d}\theta \tag{8}$$

$$E_\phi(\rho,\phi,z) = -\frac{iAC}{\pi}\int_0^{\alpha}\int_0^{2\pi}\sqrt{\cos\theta}\,\sin\theta\cos\theta\sin(\varphi-\phi)\times \\ \times J_{|m|/2}\left(\frac{\sin^2\theta}{w^2\mathrm{NA}^2}\right)\exp\left(-\frac{\sin^2\theta}{w^2\mathrm{NA}^2}\right)\exp(im\varphi)\times \\ \times\exp\left\{ik\left[z\cos\theta+\rho\sin\theta\cos(\varphi-\phi)\right]\right\}\mathrm{d}\varphi\,\mathrm{d}\theta \tag{9}$$

$$E_z(\rho, \phi, z) = \frac{iAC}{\pi}\int_0^{\alpha}\int_0^{2\pi}\sqrt{\cos\theta}\ \sin^2\theta \times$$
$$\times J_{|m|/2}\left(\frac{\sin^2\theta}{w^2\mathrm{NA}^2}\right)\exp\left(-\frac{\sin^2\theta}{w^2\mathrm{NA}^2}\right)\exp(im\varphi)\times$$
$$\times \exp\left\{ik\left[z\cos\theta + \rho\sin\theta\cos(\varphi-\phi)\right]\right\}\mathrm{d}\varphi\,\mathrm{d}\theta \tag{10}$$

The optical intensity in focal region is proportional to the modulus square of Eq. (3). It should be noted that when the topological charge of optical vortex $m = 0$, namely, E_0 is not a function of azimuthal angle φ, Eqs. (5) and (9) are equal to zero. Based on the above equations, focusing properties of radially polarized QBG beam can be theoretically investigated in detail.

3. Results and discussion

Without loss of validity and generality, it was supposed that $NA = 0.95$, $w = 1$ and $\phi = 0$. Firstly, the intensity distributions in focal region for $\mu = 1$ and different m are calculated and illustrated in Fig. 1. Here, it should be noted that the distance unit in all the figures in this paper is k^{-1}, where k is the wave number of incident beam. It can be seen that there is only one on-axis focal spot under condition of $m = 0$. And on increasing topological charge m, the focal pattern changes very considerably,

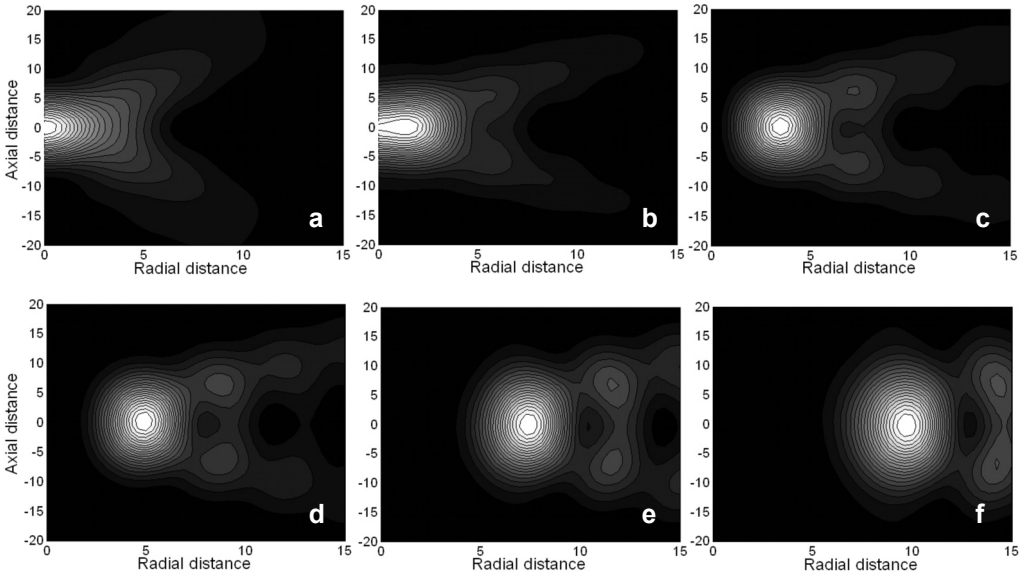

Fig. 1. Intensity distributions in focal region for $\mu = 1$ and $m = 0$ (**a**), $m = 1$ (**b**), $m = 2$ (**c**), $m = 3$ (**d**), $m = 5$ (**e**), $m = 7$ (**f**).

the intensity distribution extends in transverse direction, and one focal spot evolves into one focal plane, and then becomes one annular focal pattern, as shown in Fig. 1**b**. Increasing m continuously, this annular focal pattern goes on extending transversely, so that it changes into one focal ring, as illustrated in Fig. 1**c**. Then, the radius of the focal ring increases on increasing topological charge m, and at the same time, the width of the focal ring also broadens. From the above evolution process, we can see that the intensity distribution changes on increasing m almost in focal plane, therefore, topological charge adjusts intensity distribution more clearly in transverse direction than in longitudinal direction. The dependence of radial position of optical intensity maximum on increasing m is also calculated and shown in Fig. 2, which indicates that the dependence curve is almost linear, and m can be used to alter the size of the focal pattern.

In order to show the vector property of the field in focal region and investigate the effect of field component on total light intensity, the distributions of radial and longitudinal components under condition of $\mu = 5$ and $m = 0$ are calculated and illustrated in Fig. 3. It should be noted that the azimuthal component is zero for $m = 0$, and the other two field components are normalized by the maximum value of the total optical intensity, which can indicate the effect of the components on total intensity

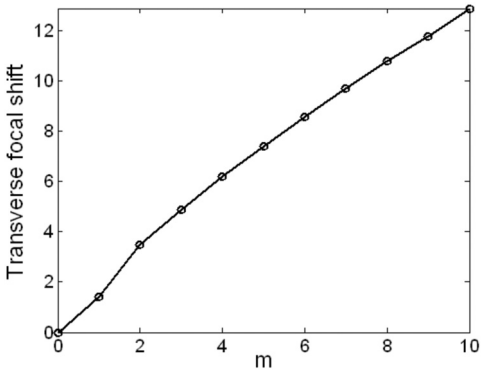

Fig. 2. Dependence of transverse focal shift on m for $\mu = 1$.

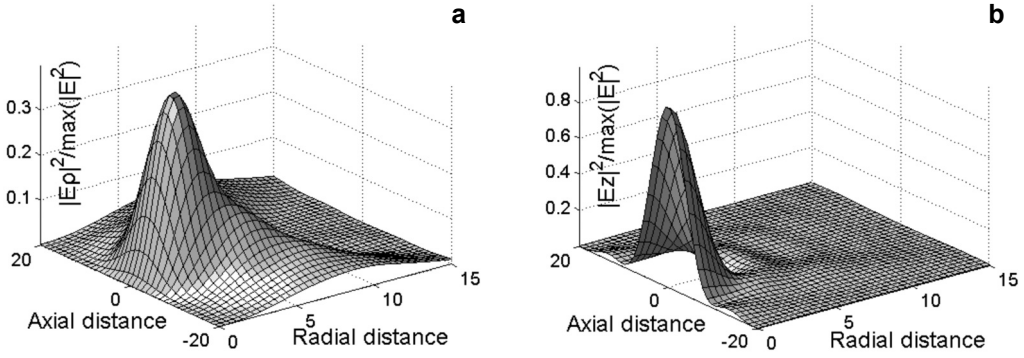

Fig. 3. The distributions of radial (**a**), and longitudinal (**b**) components in focal region under condition of $\mu = 5$ and $m = 0$.

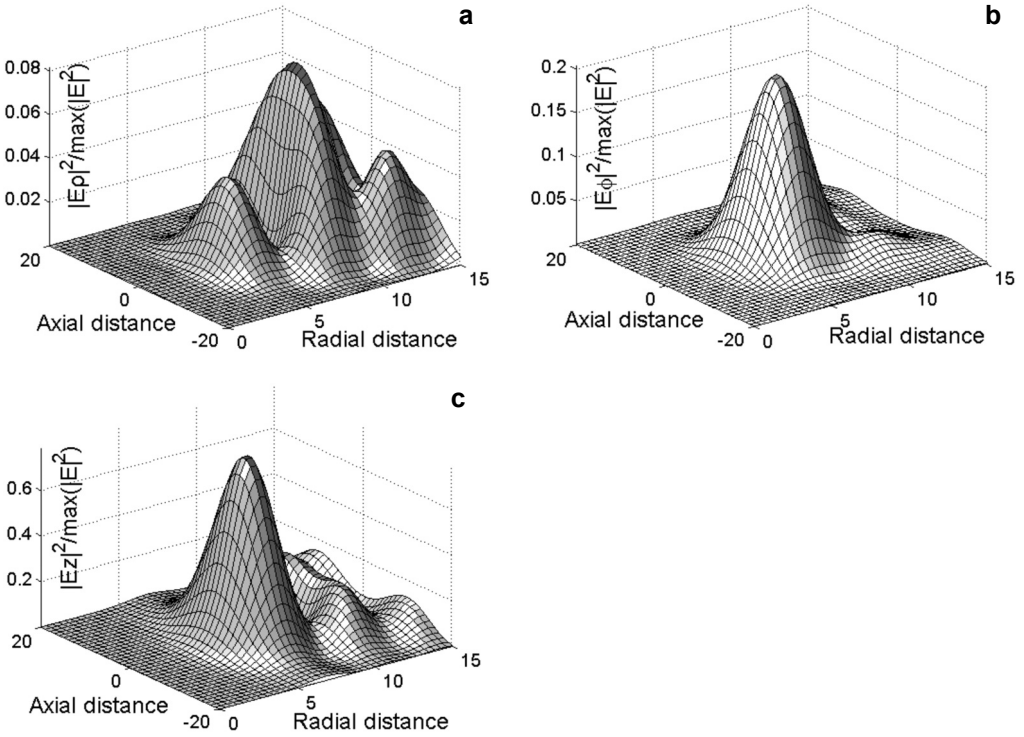

Fig. 4. The distributions of radial (**a**), azimuthal (**b**), and longitudinal (**c**) components in focal region under condition of $\mu = 5$ and $m = 5$.

distribution. From Figure 3, we can see that the longitudinal component affects the total intensity distribution more remarkably than radial component. Therefore, though the focal pattern of radial component is one ring, the maximum position of total light intensity is still on optical axis.

Figure 4 illustrates the distributions of the three orthogonal components under condition of $\mu = 5$ and $m = 5$. And the three orthogonal components are normalized by the maximum value of the total optical intensity. It can be seen that the radial component turns on multiple rings in focal region, however, this component affects the total intensity distribution more slightly than that of azimuthal and longitudinal components. And the effect of longitudinal component on total intensity distribution in focal region is the most considerable.

Then, the intensity distributions in focal region for $\mu = 3$ are investigated. Figure 5 illustrates the focal pattern evolution for $\mu = 3$. Comparing Fig. 5 with Fig. 1, it can be seen that the focal pattern changes very considerably under condition of varying beam parameter μ. The focal spot becomes flat-top focus for $\mu = 3$ and $m = 0$, and the whole focal region broadens for bigger μ, as shown in Fig. 5**a**. The position of the intensity maximum also deviates from optical axis so that the focal pattern takes on a nearly rectangular shape. On increasing m, the focal pattern becomes circular,

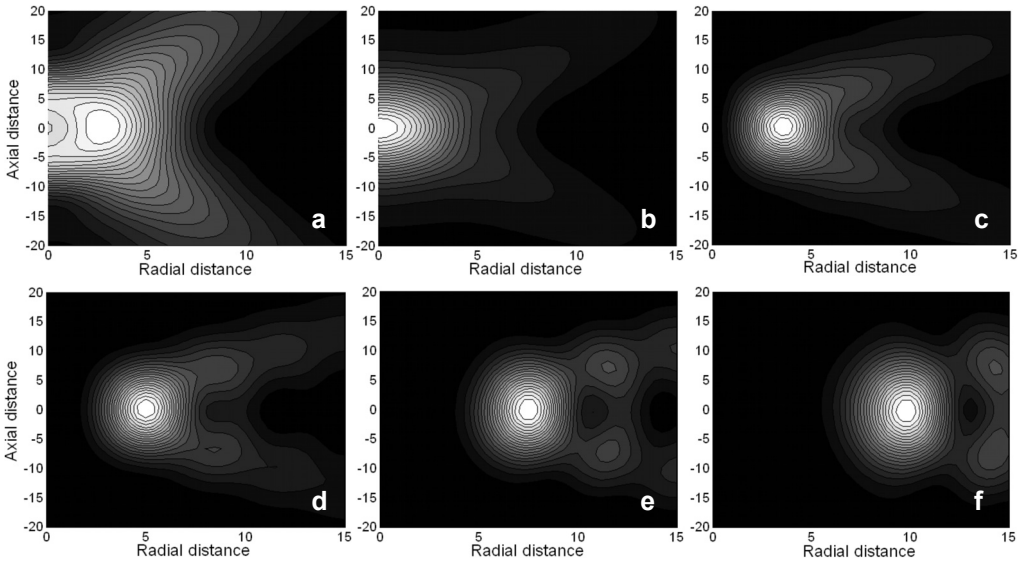

Fig. 5. Intensity distributions in focal region for $\mu = 3$ and $m = 0$ (**a**), $m = 1$ (**b**), $m = 2$ (**c**), $m = 3$ (**d**), $m = 5$ (**e**), $m = 7$ (**f**).

and the position of the intensity maximum moves back to optical axis, as illustrated in Fig. 5**b**. Increasing m continuously, one focal spot extends in transverse direction very remarkably, and changes into one focal ring, then the radius of this focal ring increases on increasing m. Therefore, the beam parameter μ can also affect intensity distribution in focal region considerably.

In order to understand the effect of the μ on focal pattern more deeply, the intensity distributions in focal region for $\mu = 5$ are also calculated and illustrated in Fig. 6. It can be seen that bigger μ can obviously alter focal pattern, and there occurs one dark hollow focus under condition of $m = 0$. The dark hollow focus is very important and desirable, for example, in optical tweezers systems, it is usually deemed that the forces exerted on the particle in light field consist of two kinds of forces, one is the optical gradient force, which plays a crucial role in constructing optical trap and its intensity is proportional to the optical intensity gradient; the other kind of force is scattering force, which usually has complex forms and whose intensity is proportional to the optical intensity [13]. Therefore, the tunable optical intensity distribution means that the controllable optical trap may occur. The dark hollow focus refers to those focuses whose optical intensity is weaker than that around it and is stable optical trap for those particles whose refractive index is smaller than that of surrounding media, and this condition is very common, especially in life science. On increasing m continuously, the dark hollow focus changes into two optical peaks along optical axis (as shown in Fig 6**b**), which can be used to construct optical traps. Focal pattern then evolves considerably from two focal peaks into two overlapping focal rings, as illustrated in Fig. 6**c**. Then, these two focal rings become more overlapping, and finally

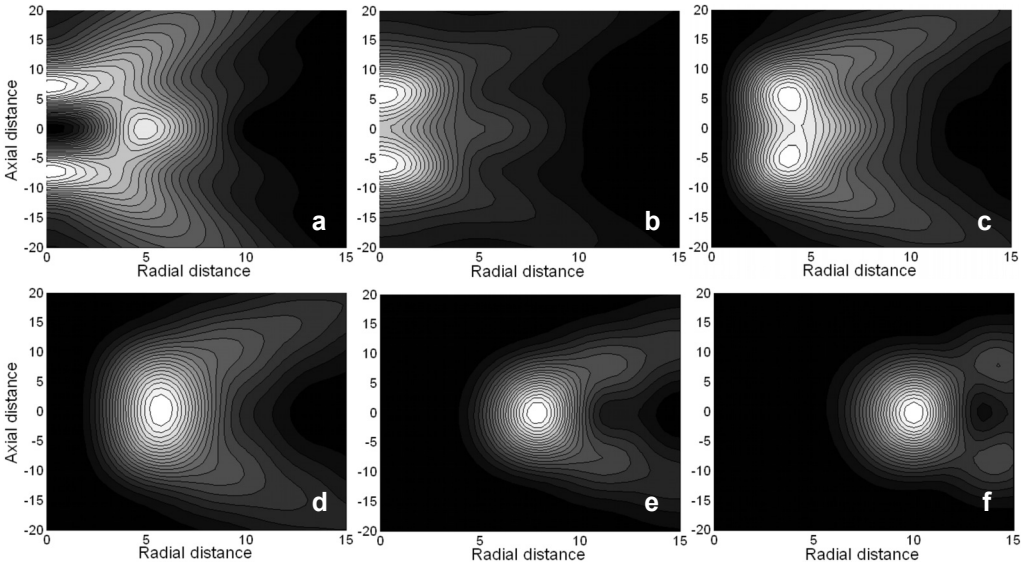

Fig. 6. Intensity distributions in focal region for $\mu = 5$ and $m = 0$ (**a**), $m = 1$ (**b**), $m = 2$ (**c**), $m = 3$ (**d**), $m = 5$ (**e**), $m = 7$ (**f**).

combine into one focal ring, and the radius of this only focal ring locating in paraxial geometrical plane broadens on increasing m.

Figure 7 illustrates the intensity distributions in focal region for bigger beam parameter $\mu = 7$. Comparing Fig. 7 with Fig. 6, we can see that the dark hollow focus

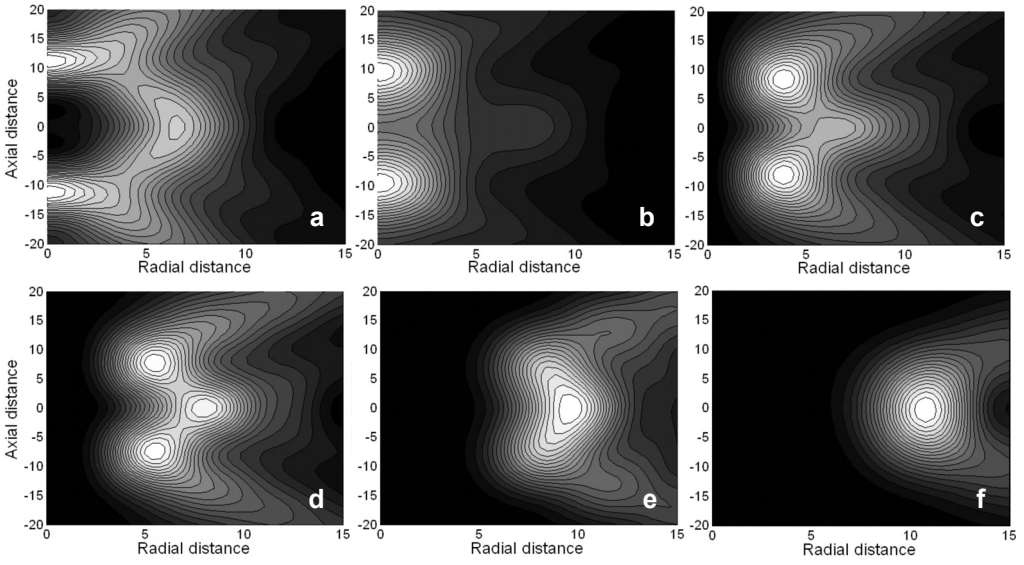

Fig. 7. Intensity distributions in focal region for $\mu = 7$ and $m = 0$ (**a**), $m = 1$ (**b**), $m = 2$ (**c**), $m = 3$ (**d**), $m = 5$ (**e**), $m = 7$ (**f**).

gets bigger under condition of higher μ. Then the dark hollow focus also changes into two optical peaks along optical axis on increasing m. However, when increasing m continuously, these two optical peaks evolve into two focal rings, then become three focal rings, which does not occur under condition of $\mu = 5$. These three focal rings become more and more overlapping, so that they combine into one focal ring, as illustrated in Fig. 7**e**. From all of the above figures, it can be seen that the focal pattern evolution principle in increasing topological charge differs obviously for varying beam parameter, especially for topological charge.

4. Conclusions

The focusing properties of radially polarized QBG beam are investigated in this paper by vector diffraction theory and simulation results show that beam parameter and the topological charge affect considerably the intensity distribution in focal region of radially polarized QBG beam. Beam parameter can induce remarkable longitudinal focal evolution, while topological charge adjusts radial intensity distribution more significantly. The focal pattern evolution principle on increasing topological charge differs obviously for varying beam parameter, especially for different topological charge. And some novel focal patterns can appear, such as two-peak focus, one-ring focus, two-ring focus, three-ring focus, and dark hollow focus, which may be used in optical trapping and manipulation systems. In addition, the effect of the field components on total intensity distribution in focal region is also different.

Acknowledgements – This work was supported by the National Basic Research Program of China (2005CB724304), National Natural Science Foundation of China (60708002, 60777045, 60871088, 60778022), the Science and Technology Commission of Shanghai Municipality (08QA14051), the Shanghai Educational Development Foundation (2007CG61), and Shanghai Postdoctoral Science Foundation of China (08R214141).

References

[1] CARON C.F.R., POTVLIEGE R.M., *Bessel-modulated Gaussian beams with quadratic radial dependence*, Optics Communications **164**(1–3), 1999, pp. 83–93.

[2] HRICHA Z., BELAFHAL A., *Focal shift in the axisymmetric Bessel-modulated Gaussian beam*, Optics Communications **255**(4–6), 2005, pp. 235–240.

[3] WANG X., LÜ B., *The beam propagation factor and far-field distribution of Bessel-modulated Gaussian beams*, Optical and Quantum Electronics **34**(11), 2002, pp. 1071–1077.

[4] BELAFHAL A., DALIL-ESSAKALI L., *Collins formula and propagation of Bessel-modulated Gaussian light beams through an ABCD optical system*, Optics Communications **177**(1–6), 2000, pp. 181–188.

[5] WANG X., LÜ B., *The beamwidth of Bessel-modulated Gaussian beams*, Journal of Modern Optics **50**(14), 2003, pp. 2107–2115.

[6] LÜ B., WANG X., *Kurtosis parameter of Bessel-modulated Gaussian beams propagating through ABCD optical systems*, Optics Communications **204**(1–6), 2002, pp. 91–97.

[7] MEI Z., ZHAO D., WEI X., JING F., ZHU Q., *Propagation of Bessel-modulated Gaussian beams through a paraxial ABCD optical system with an annular aperture*, Optik **116**(11), 2005, pp. 521–526

[8] LU F., ZHENG W., HUANG Z., *Coherent anti-Stokes Raman scattering microscopy using tightly focused radially polarized light*, Optics Letters **34**(12), 2009, pp. 1870–1871.
[9] GAO X., HU S., GU H., WANG J., *Focal shift of three-portion concentric piecewise cylindrical vector beam*, Optik **120**(11), 2009, pp. 519–523
[10] DORN R., QUABIS S., LEUCHS G., *Sharper focus for a radially polarized light beam*, Physical Review Letters **91**(23), 2003, p. 233901.
[11] TANG W.T., YEW E.Y.S., SHEPPARD C.J.R., *Polarization conversion in confocal microscopy with radially polarized illumination*, Optics Letters **34**(14), 2009, pp. 2147–2149.
[12] SATO S., KOZAWA Y., *Hollow vortex beams*, Journal of the Optical Society of America A **26**(1), 2009, pp. 142–146.
[13] VISSCHER K., BRAKENHOFF G.J., *Theoretical study of optically induced forces on spherical particles in a single beam trap I: Rayleigh scatterers*, Optik **89**, 1992, pp. 174–180.

Received September 27, 2009
in revised form January 3, 2010